



Experimental observation and analysis of the $3\nu_1(\Sigma_g)$ stretching vibrational state of acetylene using continuous-wave infrared stimulated emission

Mikael Siltanen, Markus Metsälä, Markku Vainio, and Lauri Halonen

Citation: *J. Chem. Phys.* **139**, 054201 (2013); doi: 10.1063/1.4816524

View online: <http://dx.doi.org/10.1063/1.4816524>

View Table of Contents: <http://jcp.aip.org/resource/1/JCPSA6/v139/i5>

Published by the AIP Publishing LLC.

Additional information on *J. Chem. Phys.*

Journal Homepage: <http://jcp.aip.org/>

Journal Information: http://jcp.aip.org/about/about_the_journal

Top downloads: http://jcp.aip.org/features/most_downloaded

Information for Authors: <http://jcp.aip.org/authors>

ADVERTISEMENT



Explore the **Most Cited** Collection in Applied Physics



Experimental observation and analysis of the $3\nu_1(\Sigma_g)$ stretching vibrational state of acetylene using continuous-wave infrared stimulated emission

Mikael Siltanen,¹ Markus Metsälä,¹ Markku Vainio,^{1,2} and Lauri Halonen^{1,a)}

¹Department of Chemistry, University of Helsinki, Helsinki FIN-00014, Finland

²Centre for Metrology and Accreditation, Espoo FIN-02151, Finland

(Received 13 May 2013; accepted 10 July 2013; published online 6 August 2013)

We present a sensitive experimental method for molecular spectroscopy that can be used to determine ro-vibrational states using mid-infrared stimulated emission. Our infrared stimulated emission probing (IRSEP) experiment is based on using a narrow-line, continuous-wave Ti:sapphire laser beam (pump) to excite the molecules to an upper vibrational state and a continuous-wave, mid-infrared beam from an optical parametric oscillator (probe) to detect the stimulated emission by the excited molecules. Spectroscopic data are gathered by tuning the wavelengths of the beams. The molecules are probed before their velocity distribution is disturbed by collisions, which leads to a sub-Doppler resolution. The full width at half maximum of the emission peaks is below 10 MHz. The stimulated emission lines are measured with an accuracy of at least 0.005 cm^{-1} . We use the IRSEP experiment to observe and analyze the symmetric ro-vibrational state $[21+]$ ($3\nu_1(\Sigma_g)$) of acetylene (C_2H_2). This state is not accessible via one photon transitions from the ground vibrational state. We use the least-squares method to determine that the band center is at $9991.9725(12)\text{ cm}^{-1}$ and the rotational parameters are $B = 1.156145(22)$ and $D = 1.608(87) \times 10^{-6}\text{ cm}^{-1}$, where the uncertainties in parentheses are one-standard errors in the least significant digit. © 2013 AIP Publishing LLC. [<http://dx.doi.org/10.1063/1.4816524>]

I. INTRODUCTION

Acetylene, C_2H_2 , is an extensively studied molecule in spectroscopy.¹⁻³ However, it still offers major challenges despite the large amount of conducted work. One long-standing problem concerns the symmetric vibrational states of acetylene with respect to the hydrogen nuclei permutation in the ground electronic state. The states are difficult to observe experimentally, because they are infrared inactive in one photon transitions from the ground vibrational state. In principle, Raman scattering could be used, but in practice the Raman spectra of high overtones and combinations are too weak to be observed. However, some of the symmetric states have been observed in one photon absorption as hot bands starting from asymmetric states such as the asymmetric bend $\nu_4(\Pi_u)$. These transitions are generally weak due to the unfavourable Boltzmann factor, i.e., the population of the lower state is small, requiring the use of very sensitive experimental techniques if highly excited symmetric states are the targets.⁴ There are also more sophisticated methods such as those relying on accidental perturbations induced by Stark fields,⁵ infrared laser-induced dispersed vibration-rotation fluorescence (IRLIF),⁶⁻⁸ and stimulated emission pumping (SEP) experiments.^{9,10}

The IRLIF technique has provided good observations of symmetric states of acetylene in the past.⁷ Basically, absorption of a pump beam photon gives rise to an overtone excitation of the molecules to a known, asymmetric energeti-

cally high ro-vibrational state, which can relax to a lower, symmetric state via spontaneous fluorescence. Assignment of the measured fluorescence spectrum allows the symmetric state to be analyzed. Unfortunately, the spectral resolution and thereby the accuracy of the technique is limited by the use of a dispersive instrument such as a Fourier transform infrared spectrometer. Ultimately, even with an excellent spectrometer, Doppler line broadening limits the accuracy. It is also difficult to make considerable improvements to the signal-to-noise ratio, which hinders the observation of new states with weaker fluorescence.

In this work, we use infrared stimulated emission probing (IRSEP) to observe and analyze a new symmetric state of C_2H_2 . The IRSEP technique is based on narrow linewidth, continuous-wave (cw) lasers in order to achieve high resolution. First, a cw pump laser beam is used for overtone excitation of the molecules to a rotational state of an asymmetric vibrational state. Then, a cw probe beam from a mid-infrared optical parametric oscillator brings the molecules to the symmetric vibrational state under study using stimulated emission in the mid-infrared. We directly measure a small gain in the probe beam intensity induced by the stimulated emission as a function of the probe beam frequency. This is in contrast to the typical implementation¹⁰ of a SEP experiment, where the depletion of the total fluorescence is measured using pulsed lasers and a background reference is required. Furthermore, the SEP experiment is based on electronic excitation, whereas in our case the molecules remain in the ground electronic state throughout the process. The IRSEP experiment improves the signal-to-noise ratio by over a decade compared to the IRLIF, where the spontaneous fluorescence is collisionally

^{a)} Author to whom correspondence should be addressed. Electronic mail: lauri.halonen@helsinki.fi.

dispersed over several rotational states. We chop the pump beam to modulate the excitation and stimulated emission gain of the probe beam, which both allows the high signal-to-noise ratio and eliminates the need for background zeroing or reference channel detection. In addition, our technique is Doppler-free, because the molecules are excited by a narrow linewidth pump and detected using a narrow linewidth probe.

We use the IRSEP experiment to determine the [21+] stretching vibrational state of C_2H_2 in the local mode notation.^{11–14} The corresponding normal mode notation^{15,16} is $3\nu_1$. To our knowledge, this state has not been experimentally observed before. We analyze 12 stimulated emission peaks that are measured with a typical signal-to-noise ratio of about 10 or better. We also use our technique to measure and analyze the [30+] state ($\nu_1 + 2\nu_3$ in the normal mode notation), which has been analyzed previously using the IRLIF technique.⁸ This allows us to verify the consistency of our IRSEP experiment with the earlier results. The uncertainties of the determined spectroscopic parameters agree within two-standard errors.

II. EXPERIMENTAL SETUP

The experimental setup used in this work is as follows. A high-power continuous-wave (cw) laser (Coherent Verdi V-10, 532 nm) is used to pump a single mode Ti:sapphire ring laser (Coherent 899), whose tunable, cw output beam (optical power >1 W) is used as a pump beam in the experiment. The pump beam is frequency-locked using the Pound-Drever-Hall (PDH) locking technique¹⁷ to a high finesse (>15 000) optical cavity, which simultaneously acts as a sample cell. The sample cell is built in-house and its cylinder frame is made of glass with a low thermal expansion coefficient. The implementation of the PDH locking features three feedback channels, each with different frequency ranges, and is similar to that described earlier^{18,19} with minor improvements. Drift and low frequency noise of the Ti:sapphire ring laser are corrected using a galvo actuated optical element inside the laser. The noise at frequencies from ~50 Hz to ~10 kHz is compensated by changing the optical path length of the laser's ring resonator with a piezo actuator attached to one of the laser mirrors. High frequency corrections beyond 10 kHz are provided by an acousto-optic modulator (AOM, Isomet) located outside the laser. The AOM is positioned to deflect the pump beam so that when it is turned off the beam cannot propagate to the sample cell, which provides a secondary function of chopping the beam. Sidebands needed for the PDH locking scheme are generated by passing the pump beam through an electro-optic modulator set at 10 MHz modulation frequency. A fast photodiode monitors the reflected light from the front mirror of the sample cell and thus provides the initial error signal for the PDH locking feedback loop electronics.

The optical cavity of the sample cell provides a narrow linewidth and a considerable power buildup of the pump beam laser light inside the cell. The pump beam couples to the fundamental transverse mode (TEM_{00}) of the cavity through its front mirror. The front mirror is flat and the rear mirror is con-

cave with a radius of curvature of 1 m. The free spectral range of the sample cell cavity is about 400 MHz and the reflectivities of the mirrors are over 99.98% at the wavelength of the pump laser, which gives a linewidth smaller than 25 kHz. The length of the optical cavity can be fine-tuned with a ring piezo actuator, which moves the rear mirror of the cavity. This shifts the resonance frequencies of the cavity. The frequency of the pump laser light follows the resonance frequency due to the PDH locking. Thus, the pump beam frequency can be fine-tuned on the C_2H_2 absorption peaks using the piezo actuator of the optical cavity. The optical power circulating inside the cavity reaches several hundred Watts when there is no absorption. The power usually stays above 100 W when the setup is tuned to the absorption lines used in the experiment. The optimal pressure of the C_2H_2 sample is typically between 0.1 and 0.5 Torr (1 Torr equals 101 325/760 Pa or about 1.333 mbar), because at higher pressures the measured signal decreases due to increasing collisional depopulation rate of the excited state.

The probe beam is generated using a cw optical parametric oscillator (OPO) similar to those described in Refs. 20 and 21. A frequency-tunable seed laser (Koheras, 1064 nm) is fed into an Yb-doped fiber amplifier (IPG Photonics) to provide a multi-Watt, single mode pump beam for the OPO. The OPO uses a singly resonant ring cavity configuration, where the signal beam resonates. The resonator consists of four mirrors (Quality Thin Films) in a bow-tie configuration, a periodically poled and MgO-doped (5%) lithium niobate crystal (HC Photonics) as the optically nonlinear medium, and an uncoated YAG etalon plate (0.4 mm thick) rotated by a galvo actuator for stabilization and fine frequency control. The OPO outputs a beam in the mid-infrared around 3000 cm^{-1} , which is guided through dichroic mirrors to filter out any residual light from the OPO at shorter wavelengths. The frequency of the mid-infrared output beam is coarsely set by controlling the temperature of the nonlinear crystal with thermoelectric heaters. Accurate control is achieved by rotating the YAG plate inside the resonator. During the measurements, the OPO resonator remains unchanged while the frequency of the seed laser is tuned. This method of scanning the frequency of the OPO output is continuous, i.e., without steps, and minimizes the variations in the probe beam power, profile, and pointing due to scanning. The scanning rates and ranges used in the experiment vary. Typically, these are around $0.05\text{ cm}^{-1}/\text{min}$ and about 0.05 cm^{-1} , respectively, although continuous scanning ranges of over 0.5 cm^{-1} were also achieved without problems.

The output beam from the OPO passes through a flat CaF_2 plate and the reflection is directed to a wavemeter (EXFO) and a spectrum analyzer (EXFO) used to monitor the frequency of the probe beam during the measurements. The wavemeter readout has a delay of about 1.5 s with respect to the measured signal, which is accounted for in the data analysis. The wavemeter calibration was checked using the probe beam absorption of C_2H_2 in the same sample cell, beam propagation, and detection configuration as for the actual measurements. For calibration, we use three absorption lines at 3268.48, 3275.77, and 3317.88 cm^{-1} , which have been measured earlier by others with high accuracy.²² We

found that our wavemeter readout must be corrected using an offset, which was initially $+0.0155\text{ cm}^{-1}$. The variation of the offset in a time period of a few days was at most 0.002 cm^{-1} and typically within 0.001 cm^{-1} . Within a time period of 1 month, the wavemeter readout for the same peak differed by no more than 0.004 cm^{-1} . Therefore, the accuracy of the probe beam frequency measurements is 0.005 cm^{-1} or even better. During a single measurement involving several scans of the probe beam frequency, the wavemeter readout accuracy was typically within 0.0005 cm^{-1} . Improvements in the probe beam frequency measurement would require the use of a higher resolution wavemeter, which is not at our disposal.

The mirrors of the sample cell optical cavity transmit well in the mid-infrared frequencies of the probe beam. The probe beam is directed to make a single pass through the sample cell so that the pump and probe beams are almost parallel and cross at an angle of about 0.5° in the center of the cell. The diameter of the probe beam inside the cell is about 0.6 mm. The initial power of the probe beam is close to 300 mW. We use spatial filtering with iris diaphragms, spectral filtering, and a reflection from a flat, uncoated CaF_2 plate, which decreases the beam power below 5 mW inside the sample cell. The probe beam and a small fraction (a few tens of mW) of the pump beam that leaks out of the sample cell pass through the rear mirror. These are collimated using a CaF_2 lens and are separated by a dichroic mirror. The leaked pump beam is monitored by a photodiode, whose signal is used to verify a proper PDH locking, pump beam power build-up, and sample absorption during the measurements. The probe beam is directed onto a liquid nitrogen cooled InSb detector (Infrared Associates) with a matched preamplifier. The probe beam is also spatially filtered by an iris diaphragm to reduce background noise. The experimental arrangement of the pump and probe beams, sample cell, and detectors is schematically shown in Fig. 1.

The stimulated emission due to the excited C_2H_2 molecules causes a weak gain in the probe beam at a resonance frequency. To detect it, we introduce repetitive changes in the gain by rapidly switching the pump beam on and off with the AOM in a similar manner as in high repetition rate

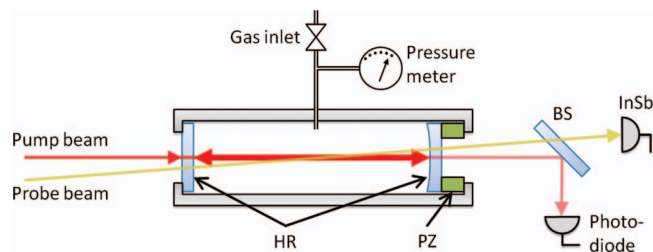


FIG. 1. A schematic representation of the experimental arrangement of the pump and probe beams, sample cell, and detectors. The symbol HR is used to mark mirrors that are highly reflecting at the pump beam frequency and transmitting in the probe beam frequency, PZ is a ring-shaped piezoelectric actuator that moves one of the mirrors, BS is a dichroic beamsplitter, and InSb is a liquid nitrogen cooled InSb detector. The pump beam is frequency locked to the optical cavity formed by the mirrors and the probe beam makes a single pass through the sample cell. The two beams cross in the middle of the cell.

cavity ring-down spectroscopy.^{18,19} As the number of excited molecules decreases, so does the gain experienced by the probe beam. It can be observed as a slight decrease of the beam intensity at the InSb detector. When the AOM is switched back on, the gain for the probe beam increases again. The probe beam intensity is monitored using a lock-in amplifier (EG&G Princeton Applied Research) with the AOM switching signal as a reference. As a result, the lock-in amplifier produces a signal which corresponds to the stimulated emission from the excited molecules. The stability of the PDH lock is a practical problem, because the lock may be lost or the pump laser may jump to another resonance frequency of the sample cell cavity during the AOM switch-off time. It has turned out that a solid PDH lock could typically be achieved by using an AOM repetition rate between 10 and 25 kHz depending on the duty cycle and the feedback loop settings. In addition, we have observed that minimizing the scattering losses of the highly reflecting front mirror of the sample cell cavity can significantly improve the stability of the PDH lock.

III. MEASUREMENT RESULTS

The measurements are performed as follows. First, the sample cell is pumped to a vacuum and then filled with fresh C_2H_2 to the desired pressure. The pump beam is tuned to the peak of a selected absorption line. The absorption is chosen so that it excites the molecules to one rotational state of the $[31-]$ vibrational state. The absorption is verified by observing the decrease of the pump beam power build-up or ring-down time in the sample cell cavity. Then, the probe beam frequency is scanned across the transition from the chosen $[31-]$ ro-vibrational state to a ro-vibrational $[21+]$ state. At the same time, the frequency of the probe beam from the wavemeter and the electric signal from the lock-in amplifier are recorded. The scan can be repeated several times using different scan rates and ranges. We have verified that the scanning direction and rate have no impact on the peak shape as a function of frequency. In addition, the scan can be repeated with the pump beam de-tuned slightly away from the center of the absorption peak, the effects of which are visible in Figs. 3 and 4 and are discussed below. We have also pumped the $[40-]$ vibrational state and probed the $[30+]$ state, which gives much stronger signal. The $[30+]$ state had been observed earlier using IRLIF and has now been used to check the consistency of our results with prior work. The vibrational states relevant to this work are schematically shown in Fig. 2 along with their energies in cm^{-1} above the ground vibrational state.

A typical lock-in amplifier signal as a function of time during the scan across the transition to the $[21+]$ vibrational state is shown in Fig. 3(a). The lock-in amplifier integration time is 30 ms and the sensitivity is 1 mV. An overlay of several scans as a function of frequency with various amounts of pump beam frequency de-tuning is composed in Fig. 3(b). Wavemeter data are used to obtain the horizontal axis. The resolution is limited by the linewidth of the probe beam. The OPO resonator is not frequency locked and, therefore, we

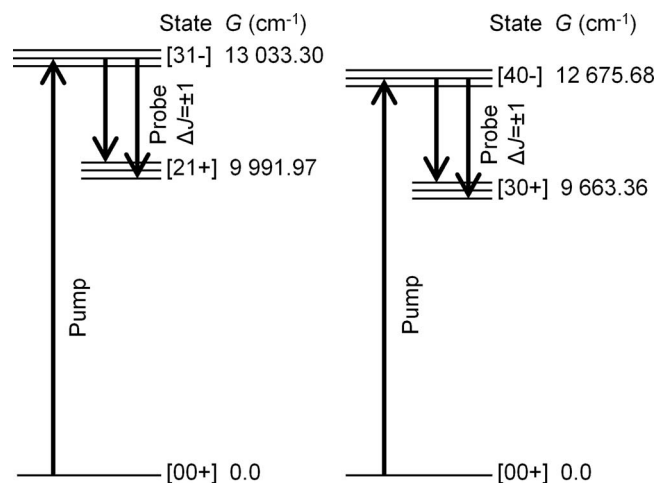


FIG. 2. An energy level diagram showing the vibrational energies of acetylene with pump and probe transitions used in the IRSEP experiment. The probe transition is measured using stimulated emission. The vibrational term values are labeled with the symbol G .

measured the probe beam linewidth to be of the order of 1 MHz in the timescale of 1 s.

Several interesting properties are visible in Fig. 3. The features show up in the measurements repeatedly. In order to verify the reliability of the measurement system, we checked that the shape and position of the peaks do not depend on the scanning rate, scanning direction, or the optical intensity of the probe beam. The signal approaches zero as the probe beam frequency is tuned away from the peak indicating zero offset due to background. In other words, a separate scan or zeroing for determining the background signal level is unnecessary. A visible property is the appearance of two narrow (full width at half maximum is below 10 MHz) peaks instead of one in a single scan. The measured linewidths of the peaks are believed to be close to the actual linewidths, because the probe beam bandwidth is 1 MHz or less. The measured peak linewidths are close to the pressure broadened values as estimated by others in similar sample conditions.²³ Measurements as a function of pressure and probe beam power indicate that other linewidth broadening mechanisms (natural, power, transit time) also contribute to our measurement, but these are estimated to be less significant. A close examination of the peaks also reveals that in many measurements the peak tails are asymmetric. The origin of the asymmetry is not fully clear. Therefore, an effect caused by the experimental arrangement cannot be ruled out.

The appearance of the two narrow peaks is a result of the excitation by a narrow-line laser light within the optical build-up cavity. If the pump beam frequency is de-tuned from the center of the absorption peak, only the molecules with a Doppler shift matching the amount of de-tuning are excited. The pump beam forms a standing wave, where light propagates in both forward and backward directions along the beam. Thus, two groups of molecules with velocity components matching the Doppler shift (equal in magnitude but in opposite directions) along the beam are excited. The probe beam frequency must also match the Doppler shift of the excited molecules in order for the stimulated emission to

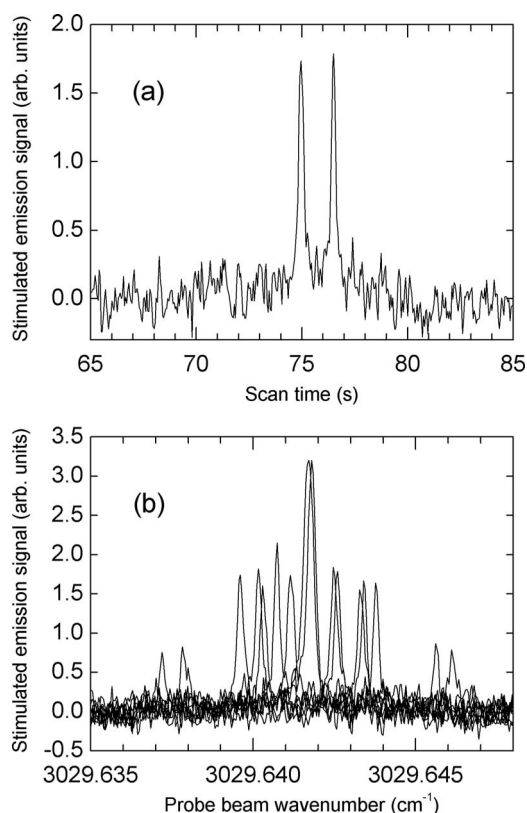


FIG. 3. (a) A typical measurement signal as a function of time. The pump beam frequency is fixed at the absorption with a small amount of de-tuning from the absorption peak center. The probe beam frequency is scanned across the transition to the final symmetric vibrational state while the stimulated emission signal is recorded. Two peaks are observed as a result of non-zero de-tuning of the pump beam. (b) An overlay of nine scans as a function of the measured wavenumber of the probe beam. The amount of pump beam de-tuning is varied between successive scans, which results in several pairs of symmetrically located signal peaks. The distances of the peaks from the center increases with the amount of de-tuning. When the amount of de-tuning is zero, the peaks coincide and double the signal intensity. The pressure of the sample in both (a) and (b) is between 0.1 and 0.2 Torr.

occur. Therefore, if the velocity components of the excited molecules along the beam path do not change notably, the probe beam is at resonance when its frequency is offset by the amount of pump beam de-tuning in either positive or negative direction. This leads to two narrow Lorentzian peaks located symmetrically around the center of the transition. When the pump beam frequency is at the center of the absorption peak, the excited molecules have no Doppler shift. The two peaks in the stimulated emission signal overlap at the exact frequency of the transition as expected. In our experiment, the linewidths of the two peaks remain sub-Doppler and close to the expected value due to pressure broadening.²³ This indicates that, on the average, the excited molecules experience only few collisions that change their velocity before they are probed.

All measured transitions that are used to determine the newly observed symmetric $[21+]$ state are chosen so that the total angular momentum quantum number is preserved while the molecule is in the intermediate antisymmetric $[31-]$ state after excitation by the pump beam. In other words, we effectively exclude rotationally inelastic collisions. In this way,

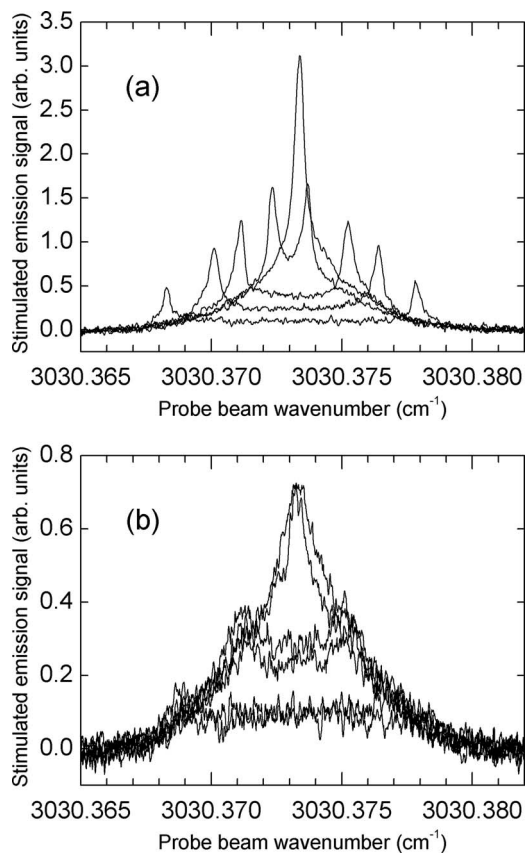


FIG. 4. Overlay of the stimulated emission signal when the upper intermediate state is populated via collisions. The molecules are first pumped to the upper, intermediate vibrational state [40−]. Then, the transition to the final [30+] vibrational state is probed using stimulated emission. Before probing the transition, molecular collisions have changed the total angular momentum quantum number J of the upper, intermediate ro-vibrational state by -2 and -4 in (a) and (b), respectively. The sample pressure in both (a) and (b) is about 0.1 Torr.

the line broadening is minimized and the measured signal intensity is maximized. We also observed and measured some transitions involving a change of the total angular momentum quantum number in the intermediate rotational state due to collisions after the pump beam excitation. When pumping the [31−] vibrational state, the transitions from these rotational states populated by collisions give such a weak signal that finding the peaks experimentally is difficult.

When pumping the [40−] state instead of the [31−] state, the stimulated emission from the collision-populated states can be observed due to a more efficient excitation. The peak shapes observed in this case with a varying amount of pump beam de-tuning are shown in Fig. 4(a). The two narrow Lorentzian peaks can still be distinguished and are separated in frequency due to a finite amount of pump beam de-tuning during the excitation. Additionally, the signal level is now non-zero in between or surrounding the Lorentzian peaks, depending on their separation, because the collisions have changed the velocities and Doppler shifts of a large fraction of the molecules. The velocity distribution of the molecules is partially randomized towards a Gaussian, Doppler-broadened distribution. The broadened lineshape cannot be readily fitted using a simple combination of basic lineshape functions,

which suggests that successful simulation of the lineshapes might provide additional information regarding the molecular collisions. However, such task is beyond the scope of this work. In Fig. 4(b), the collision-induced changes in the total angular momentum and the velocity distribution of the molecules are larger than in Fig. 4(a). Because of a higher number of collisions, the distribution changes further towards Gaussian. The overall signal level decreases, since the excited molecules tend to be re-populated amongst a large number of rotational states with increasing number of collisions. The molecules also eventually drift away from the measurement volume before reaching an equilibrium in rotational energy.

The definition used for the signal-to-noise ratio (SNR) is the ratio of the height of the stimulated emission peaks with slightly de-tuned pump beam and the standard deviation of the signal noise without the peaks. When measuring the transitions leading to the newly observed [21+] vibrational state, the SNR is typically around 10 or better. Transitions leading to the [30+] vibrational state were characterized previously using the IRLIF technique with the SNR of the highest peaks in the FTIR data being of the order of 100. For those transitions, our IRSEP experiment reaches SNR values of well over 500. When the Doppler shift is zero, the two peaks coincide doubling the peak height leading to the SNR of over 1000.

The observed frequencies of the stimulated emission peaks were each determined using a measurement consisting of several linear scans of the probe beam frequency. The amount of de-tuning of the pump beam from the center of the absorption line was varied between the scans. The measured wavenumbers of the stimulated emission peaks of transitions leading to the [21+] state are listed in Table I along with the corresponding wavenumbers of the absorption lines to which the pump beam was tuned. The total angular

TABLE I. Transition wavenumbers of C_2H_2 leading to the [21+] vibrational state measured using the IRSEP technique. We first excite the molecules with the pump laser from the ground vibrational state to the [31−] state and then bring them to the [21+] state via stimulated emission by the probe laser. The quantities J'' and J' are the total angular momentum quantum numbers of the initial (ground) and final ro-vibrational states, respectively. The quantity ν_{pump} is the wavenumber²⁴ of the center of the absorption peak used for excitation by the pump beam. The quantity ν_{se} is the center wavenumber of the measured stimulated emission peaks. The quantity $\nu_{\text{obs}} - \nu_{\text{calc}}$ is the difference between the observed and calculated wavenumbers obtained from data analysis as explained in Sec. IV.

J''	J'	$\nu_{\text{pump}} \text{ (cm}^{-1}\text{)}$	$\nu_{\text{se}} \text{ (cm}^{-1}\text{)}$	$\nu_{\text{obs}} - \nu_{\text{calc}} \text{ (cm}^{-1}\text{)}$
5	3	13 020.9999	3050.451	0.00083
5	5	13 020.9999	3029.642	0.00094
9	7	13 010.2227	3059.399	−0.00287
9	9	13 010.2227	3020.096	−0.00082
10	8	13 007.3986	3061.603	0.00043
10	10	13 007.3986	3017.682	−0.00097
11	9	13 004.5212	3063.797	0.00067
11	11	13 004.5212	3015.255	−0.00044
13	11	12 998.6127	3068.151	0.00185
13	13	12 998.6127	3010.370	0.00083
15	13	12 992.4925	3072.456	0.00032
15	15	12 992.4925	3005.440	−0.00076

momentum quantum numbers of the initial and final states are also listed.

The continuous scanning range of the probe beam of less than 1 cm^{-1} does not allow for more than one stimulated emission peak to be measured at one time. Unfortunately, minor changes in the detection equipment and optical alignment after re-setting the frequencies of the pump and/or probe beams can have a noticeable effect on the detected peak height. In addition, the absolute power and intensity noise properties of the probe beam can vary from one measurement run to another as the OPO wavelength setting needs to be changed. Therefore, an accurate determination of the intensities of the stimulated emission peaks on a unified scale is impossible.

IV. ROTATIONAL ANALYSIS OF THE [21+] VIBRATIONAL STATE

Using the IRSEP technique, we have accessed a symmetric vibrational state [21+] in the local mode notation where the quantum numbers refer to the two identical CH stretching oscillators.^{11,12,14} In the standard normal mode picture, the assignment is $3\nu_1$.¹⁵ In the experiment, starting from the ground vibrational state, we have pumped the [31−] state at $13\,033.3\text{ cm}^{-1}$ and then probed the energy difference of [31−] and [21+] at 3041.3 cm^{-1} . We have pumped altogether 6 rotational states of [31−] via P branch transitions ($\Delta J = J' - J'' = -1$), J'' ranging from 5 to 15. We have observed both of the possible $\Delta J = \pm 1$ transitions with the probe laser. The energy differences between pump and probe laser transitions depend only on the spectroscopic parameters of the [21+] and the ground state. The energies have been modelled with the basic energy level formula¹⁵

$$\frac{E}{hc} = G + F(J) = G + BJ(J+1) - DJ^2(J+1)^2 + HJ^3(J+1)^3, \quad (1)$$

where G is the vibrational term value and B , D , and H are rotational parameters of different vibrational states. The parameter H is fixed to zero in all other cases except the ground state. The ground state rotational parameters have been fixed to $B = 1.17664686$, $D = 1.62754 \times 10^{-6}$, and $H = 1.674 \times 10^{-12}\text{ cm}^{-1}$.²⁵ We have determined the vibrational term value $9991.9725\text{ (12)}\text{ cm}^{-1}$ and the rotational parameters $B = 1.156145\text{ (22)}$ and $D = 1.607\text{ (87)} \times 10^{-6}\text{ cm}^{-1}$ of the [21+] state with the linear least squares method using our measured transition wavenumbers as data (the pump laser transition wavenumbers from Ref. 24 minus our probe laser wavenumbers). The numbers in parentheses indicate one-standard errors in the least significant digit.

The standard deviation of the linear least squares fit, $1.4 \times 10^{-3}\text{ cm}^{-1}$, most likely reflects the precision of the measurements. This agrees well with our long term (even over 1 month) wavenumber measurements of several induced emission lines with the wavemeter. The accuracy is a bit more difficult to estimate. First, we have remeasured 8 transitions associated with the vibrational state [30+].⁸ The band origin obtained by us is $9663.362\text{ (16)}\text{ cm}^{-1}$ (one-standard error). In

this analysis, some of the stimulated emission peak wavenumbers had to be extracted from early data collected during the development of our optical setup, when the system was not yet optimized. For example, the mirrors of the sample cell cavity had to be replaced with new ones to minimize optical losses and thermal effects at the mirror surfaces. Therefore, the precision of the analysis is not as good as in the case of the data used for the analysis of the [21+] vibrational state. Nevertheless, the determined band origin can be compared with the value $9663.3860\text{ (11)}\text{ cm}^{-1}$, which has been estimated to be accurate within 0.01 cm^{-1} .⁸ The band origins and the corresponding rotational parameters agree within two-standard errors. Second, as explained in Sec. II, we have constantly checked the accuracy of our wavemeter during the emission measurements with three accurately known acetylene absorption lines²² at 3317.88 , 3275.77 , and 3268.48 cm^{-1} and come to the conclusion that the accuracy of our stimulated emission measurement is 0.005 cm^{-1} or better.

The results we have obtained can be compared with simple local mode models and calculations. If the CH stretching oscillators were uncoupled from each other, then the states such as [30+] and [30−] would have the same vibrational term values and rotational parameters. A similar conclusion applies to the [21+] and [21−] states. In molecules with coupled CH oscillators, the same occurs in the case of highly excited CH stretching vibrational states, where the bond oscillators become effectively uncoupled due to the anharmonicity.^{11,12,26} In practice, in the case of the [30+] state, the band origin is 9663.39 cm^{-1} and the rotational constant is 1.1580 cm^{-1} .⁸ In comparison, for the [30−] state, the corresponding values are 9639.85 and 1.1584 cm^{-1} .²⁷ For the [21+] state, the band origin is 9991.97 cm^{-1} and the rotational constant is 1.1561 cm^{-1} , whereas for the [21−] state the corresponding values are 9835.16 and 1.1576 cm^{-1} .²⁷ As expected, by looking at the vibrational correlation diagrams between the local and normal mode limit, the [21+] and [21−] states are less localised, i.e., the differences between the band origins and rotational constants are larger than in the case of the [30+] and [30−] states.^{11,12} A very pleasing finding is the excellent agreement between our newly observed vibrational term value 9991.97 cm^{-1} of the [21+] state and the computed one 9988.96 cm^{-1} ,¹⁶ taking into account the simplicity of the coupled stretching vibrational anharmonic bond oscillator local mode model employed in Ref. 16.

V. CONCLUSIONS

To summarize, we have developed an IRSEP experiment and applied it to obtain new spectroscopic data on symmetric ro-vibrational states of gaseous C_2H_2 in the ground electronic state. We observe the symmetric [21+] vibrational state of C_2H_2 in the local mode notation ($3\nu_1$ in the normal mode notation). To our knowledge, this state has not been observed earlier. We analyze the state with the least squares method using the measured wavenumbers of the stimulated emission peaks as data. From the analysis, we determine the vibrational term value $9991.9725\text{ (12)}\text{ cm}^{-1}$ and the rotational parameters $B = 1.156145\text{ (22)}$ and $D = 1.608\text{ (87)} \times 10^{-6}\text{ cm}^{-1}$. We also used the IRSEP experiment to measure and analyze

the [30+] vibrational state ($\nu_1 + 2\nu_3$ in the normal mode notation) to confirm the agreement with earlier results obtained using infrared laser induced dispersed fluorescence technique. These results agree within two-standard errors. The measured linewidths of the stimulated emission are sub-Doppler and the signal-to-noise ratio is an order of magnitude better compared to the earlier data obtained using the fluorescence technique. In this work, we use acetylene as the sample molecule, although the IRSEP experiment is expected to be applicable to other molecules as well.

ACKNOWLEDGMENTS

The authors would like to gracefully acknowledge the financial support from the Academy of Finland.

- ¹M. Herman, J. Liévin, J. Vander Auwera, and A. Campargue, *Adv. Chem. Phys.* **108**, 1 (1999).
²M. Herman, A. Campargue, M. I. El Idrissi, and J. Vander Auwera, *J. Phys. Chem. Ref. Data* **32**, 921 (2003).
³B. J. Orr, *Int. Rev. Phys. Chem.* **25**, 655 (2006).
⁴S. Kassi and A. Campargue, *J. Chem. Phys.* **137**, 234201 (2012).
⁵J. A. Barnes, T. E. Gough, and M. Stoer, *Chem. Phys. Lett.* **237**, 437 (1995).
⁶P. Jungner and L. Halonen, *J. Chem. Phys.* **107**, 1680 (1997).
⁷M. Saarinen, D. Permogorov, and L. Halonen, *J. Chem. Phys.* **110**, 1424 (1999).

- ⁸M. Metsälä, S. Yang, O. Vaaitinen, and L. Halonen, *J. Chem. Phys.* **117**, 8686 (2002).
⁹C. E. Hamilton, J. L. Kinsey, and R. W. Field, *Annu. Rev. Phys. Chem.* **37**, 493 (1986).
¹⁰C. Kittrell, E. Abramson, J. L. Kinsey, S. A. McDonald, D. E. Reisner, R. W. Field, and D. H. Katayama, *J. Chem. Phys.* **75**, 2056 (1981).
¹¹M. S. Child and R. T. Lawton, *Faraday Discuss. Chem. Soc.* **71**, 273 (1981).
¹²M. S. Child and L. Halonen, *Adv. Chem. Phys.* **57**, 1 (1984).
¹³J. M. Mills and A. G. Robiette, *Mol. Phys.* **56**, 743 (1985).
¹⁴L. Halonen, *Adv. Chem. Phys.* **104**, 41 (1998).
¹⁵G. Herzberg, *Infrared and Raman Spectra of Polyatomic Molecules* (Van Nostrand, New York, 1945).
¹⁶L. Halonen, M. S. Child, and S. Carter, *Mol. Phys.* **47**, 1097 (1982).
¹⁷R. W. P. Drever, J. L. Hall, F. V. Kowalski, J. Hough, G. M. Ford, A. J. Munley, and H. Ward, *Appl. Phys. B* **31**, 97 (1983).
¹⁸R. Z. Martinez, M. Metsälä, O. Vaaitinen, T. Lantta, and L. Halonen, *J. Opt. Soc. Am. B* **23**, 727 (2006).
¹⁹M. Metsälä, J. Guss, O. Vaaitinen, R. Z. Martinez, and L. Halonen, *Chem. Phys. Lett.* **424**, 7 (2006).
²⁰A. Henderson and R. Stafford, *Opt. Express* **14**, 767 (2006).
²¹M. Vainio, J. Peltola, S. Persijn, F. M. J. Harren, and L. Halonen, *Opt. Express* **16**, 11141 (2008).
²²J. Vander Auwera, D. Hurtmans, M. Carleer, and M. Herman, *J. Mol. Spectrosc.* **157**, 337 (1993).
²³J. Ye, Ph.D. thesis, University of Colorado, Boulder, 1997, pp. 167.
²⁴J. Sakai and M. Katayama, *J. Mol. Spectrosc.* **154**, 277 (1992).
²⁵C. S. Edwards, G. P. Barwood, H. S. Margolis, P. Gill, and W. R. C. Rowley, *J. Mol. Spectrosc.* **234**, 143 (2005).
²⁶T. Lukka and L. Halonen, *J. Chem. Phys.* **101**, 8380 (1994).
²⁷M. Herman, T. R. Huet, and M. Vervloet, *Mol. Phys.* **66**, 333 (1989).